Journal of Photochemistry and Photobiology 8 (2021) 100089

Contents lists available at ScienceDirect

Journal of Photochemistry and Photobiology

journal homepage: www.sciencedirect.com/journal/journal-of-photochemistry-and-photobiology

Enhancing fluorescence and lowering the optical gap through C═P doping of a π-conjugated molecular backbone: A computational-based design approach

Sunandan Sarkar [a], Pandiselvi Durairaj [a], John D. Protasiewicz [b], Barry D. Dunietz [*,c]

[a] Department of Chemistry, National Institute of Technology, Tiruchirappalli, Tamil Nadu 620015, India
[b] Department of Chemistry, Case Western Reserve University, Cleveland, Ohio 44106, USA
[c] Department of Chemistry and Biochemistry, Kent State University, Kent, Ohio 44242-0001, USA

ARTICLE INFO

Keywords:
Fluorescence
Benzoxaphosphole
Material design
Phosphaalkene
Excited states

ABSTRACT

Design principles of organic fluorescent materials are investigated at the molecular level using a first-principles-based computational approach. The design approach incorporates hetero atoms into a conjugated cyclic skeleton by introducing C═P bonds. In particular we report the design of a molecular system of an extended conjugation system that maintains its planarity across the full system, achieving low lying electronic excited states of large oscillator strengths. We also present calculations that confirm the competing process of internal system crossing to be too slow for affecting the actual relaxation following photexcitation.

1. Introduction

Organic materials bear potential to advance optoelectronic applications through their biocompatibility and tunability of their optical properties [1–5]. In particular organic fluorescent materials are used in light-emitting devices, [6–9] where efforts to improve conversion efficiencies are pursued [10–13]. In this direction vast efforts are directed to find organic fluorescents that are associated with electronic excitations in the IR and near IR spectral regions [14–17]. Materials properties can be tuned to control their emissivity including through electrical input [18]. To enhance the solid state emission using organic materials, [19–21] the design efforts tend to focus on the intermolecular forces [22, 23]. In a more direct approach, the molecular design addresses the optoelectronic gap of conjugated systems [24,25]. Modification of the organic conjugated system can be employed to control luminescence properties, [26] for example, number and position of alkoxy substituents and alkyl chain length direct the molecular packing and consequently their fluorescence properties in diphenylbutadienes. However, employing such bottom-up perspective for the discovery of low orbital gap organic fluorescent materials[27] remains underutilized.

The goal of the reported research is to delineate design principles of materials that exhibit enhanced photoluminescence using molecular level modifications. The design approach is based on doping a conjugated system by incorporating hetero-atoms into the conjugation skeleton [28–31] combined with the proper increase of the conjugation system. While incorporating C=P bonds appears to only marginally affect the photoluminescence over that of the parent conjugated material, [31–36] some exceptions of significant photoluminescence have been indicated. [37–48] For example, 2-phenyl-1,3-benzoxaphosphole (R-BOP, in Fig. 1, where R is a phenyl group) exhibits efficient fluorescence while the analogous unfunctionalized molecule (R=H) appears to be inactive [39]. Organic materials consisting of multiple C═P bonds, e.g., Ph_2-NBOP and BisBOP-Np molecules (also shown in Fig. 1) presenting significant luminescence were also reported [40,41].

Recently, we have established structure-fluorescence relationships in organophosphorus compounds [49]. We have shown that the planarity of π-extended systems is essential for exhibiting bright fluorescence. In addition, the optical gap was shown to depend on the π-conjugation, decreasing with the increase of the system size. While computation efforts on related P═C materials have recently been reported, [50,51] our approach addresses effectively singlet-triplet gaps that are essential for the study of quantum yields of excited state luminescence. In this work, we present using a computational approach design principles of organic materials that contain multiple C═P bonds and which are associated with bright fluorescence and a reduced optical gap. We choose the Ph_2-NBOP system as the kernel compound, where we functionalize it with two additional BOP units at 3,7 positions of the fused naphthalene. This derived form is addressed below as FA-BOP (see illustrated below in

* Corresponding author.
E-mail addresses: ssarkar@nitt.edu (S. Sarkar), bdunietz@kent.edu (B.D. Dunietz).

https://doi.org/10.1016/j.jpap.2021.100089
Received 30 July 2021; Received in revised form 9 November 2021; Accepted 16 November 2021
Available online 20 November 2021

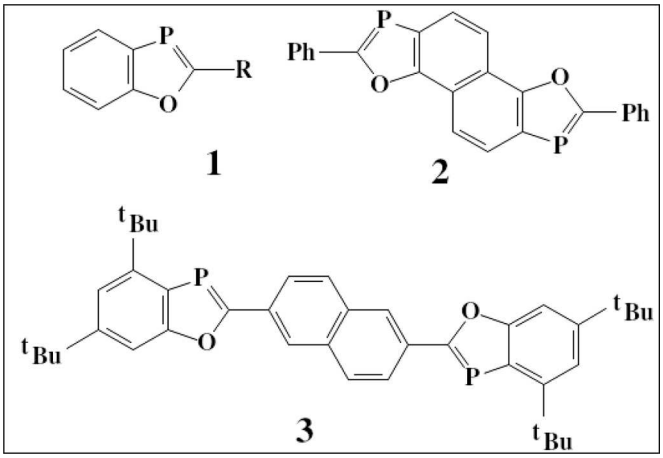

Fig. 1. Luminescent organic materials of benzoxaphosphole derivative with C=P bonds (**1** R-BOP, **2** Ph_2-NBOP and **3** BisBOP-Np) [39–41].

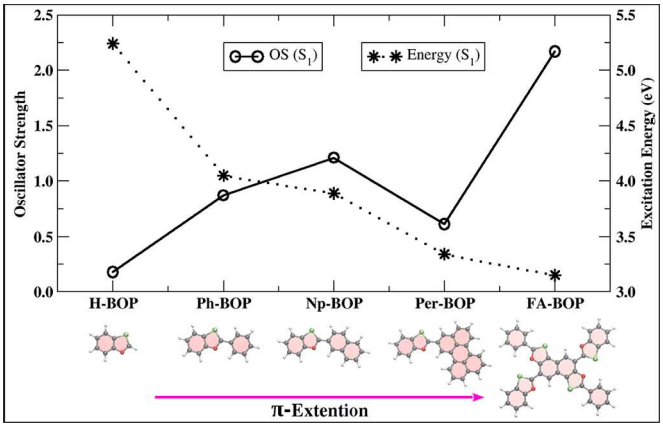

Fig. 2. A series of R-BOP systems, in the order of increasing conjugated system. The considered series correspond to materials where R is hydrogen (H), benzene (Ph), naphthalene (Np), and perylene (Per). Also shown is the proposed FA-BOP that features an extended conjugated skeleton of multiple BOP units. The calculated trends of the red-shifting of the excitation energy are shown by the black dotted line, and of the oscillator strength that is overall increased with the noted drop for Per-BOP by the black solid line. (For interpretation of the references to colour in this figure legend, the reader is referred to the web version of this article.)

Fig. 2).

2. Methods and computational approach

The fluorescence (FL) efficiency or quantum yield [52] (Φ_{fl}) is determined as the relative weight of the radiative decay (k_{fl}) of the total deactivation that includes non radiative processes (k_{nr}):

$$\Phi_{fl} = \frac{k_{fl}}{k_{fl} + k_{nr}}. \tag{1}$$

The lowest singlet excited state can be deactivated through non radiative competing processes including internal conversion to the ground state, energy dissipation through coupling to the molecular environment, and intersystem crossing (ISC) to triplet states. Here, we assume that the ISC dominates the non-radiative pathways within uni-molecular photophysics[53] as observed for solvated oligothiophenes and polythiophenes [54–57].

The FL rate constant (k_{fl}) is determined by a simplified and widely used version of the Strickler-Berg equation: [58,59]

$$k_{fl} = 0.6671\left[cm^2 s^{-1}\right]\frac{\nu_{em}^3}{\nu_{ab}} n^2 f, \tag{2}$$

where ν_{ab} and ν_{em} are the frequencies (in cm^{-1}) corresponding to the absorption and emission energies, and n is the refractive index of the solvent, and f is the oscillator strength (OS) of the emitting excited state at the excited state geometry. The OS is proportional to the square of transition dipole moment, $f \propto |\vec{\mu}_{01}|^2$. [60]

The ISC rate constant (k_{isc}) for the transition between the lowest singlet excited state (S_1) and a triplet excited state (T_m) is obtained by the Marcus rate expression for a thermally activated process [61–63]:

$$k_{isc} = \frac{\left|V^{soc}_{(T_m,S_1)}\right|^2}{\hbar}\sqrt{\frac{\pi}{k_B T \lambda}}\exp\left[-\frac{(\lambda + \Delta G)^2}{4\lambda k_B T}\right]. \tag{3}$$

Here $V^{soc}_{(T_m,S_1)} \equiv \langle T_m|\mathbf{H}_{SO}|S_1\rangle$ is the spin-orbit coupling matrix element, λ is the reorganization energy (i.e., the energy difference of T_m state at S_1 minima and T_m minima), and ΔG is the free energy difference between the T_m and the S_1 minima. Below we confirm that all the considered processes follow the normal regime of $|\Delta G| < \lambda$, where the semiclassical limit is reliably applicable [61].

We use density functional theory (DFT) to calculate ground state properties, and the Tamm-Dancoff approximation (TDA) of the time-dependent DFT (TDDFT) to obtain excited states properties [64–67]. The range-separated hybrid (RSH) ωB97X-D functional, [68–70] which accounts for long-range Coulomb and dispersion interactions, and the 6-31G(d,p) basis set are used in all calculations unless noted otherwise. The larger 6-311^{++}G(d,p) basis set is used to confirm convergence of the excitation energy and its OS. The polarizable continuum solvation model (PCM) is applied with a dielectric constant 8.93 and refractive index 1.425 to represent the di-chloromethane solvent. The spin-orbit coupling elements are obtained within TDA calculations [62]. We employed the state-tracking algorithm to optimize the geometries of excited triplet states that are addressed as the acceptor states in the competing transition to the radiative processes [71]. All the calculations were performed using Q-Chem 4.4 package [72].

3. Results and discussion

We first examine the absorption properties of a series of R-BOP systems. The S_1 state of the R-BOP systems are dominated by HOMO-LUMO transition (H → L). As illustrated in Fig. 2, the calculated S_1 energy shows the expected trend, where it decreases from 5.24 eV for H-BOP to 3.34 eV for Per-BOP reflecting the increased size and delocalization of the π-system (see the 6-31G(d,p) values listed in Table 1). The OS of the S_1 state also follows the expected trend, where it increases from H-BOP at 0.18 to Np-BOP with 1.21, but then demonstrates a

Table 1
Calculated absorption energies (E_{ab}) of the lowest singlet excited state (S_1), oscillator strengths (f) and dominant molecular orbital replacements with the amplitude.

R-BOP	E_{ab} (eV)	f	MO involvement
		6-31G(d,p)	
H-BOP	5.24	0.18	H → L (0.86)
Ph-BOP†	4.05	0.87	H → L (0.97)
Np-BOP	3.89	1.21	H → L (0.96)
Per-BOP	3.34	0.61	H → L (0.94)
		6–311+G(d,p)	
H-BOP	5.13	0.23	H → L (0.92)
Ph-BOP	3.97	0.85	H → L (0.97)
Np-BOP	3.83	1.20	H → L (0.96)
Per-BOP	3.24	0.60	H → L (0.95)

† The measured absorption maximum of Ph-BOP is 337 nm (3.68 eV) [39].

deviation from the expected trend, where it drops for Per-BOP to 0.61.

In considering the trend of the excited state properties shown in Fig. 2 the increase of the conjugation system as achieved in Per-BOP is not associated with the expected enhanced delocalization. We point out that the substitution position in Per-BOP is the same position as in the considered molecules in the series. For completeness we also addressed a structural isomer of Per-BOP, which is functionalized at other positions at the 3-position of Per, that is the expected chemically active position. See the two conformational isomers of 3-Per-BOP in SI Figure S1. As indicated in the Figure, the lower conformation 3-Per-BOP energy is less stable than Per-BOP by 2.4 kcal/mol. We relate this trend of relative stability to intramolecular repulsion, where 3-Per-BOP becomes non-planner with a dihedral angle between the BOP and Per planes of around 40° We also point out that the S_1 state which is red-shifted by about 0.2-0.3 eV and with higher OS (1.28 and 1.33) compared to the Per-BOP.

To further explain the OS trends of the low lying singlet excited state, S_1, we consider the associated natural transition orbitals (NTOs). We confirm the hole and electron NTOs pair to be well delocalized in the case of Np-BOP. The transition dipole moment of the Np-BOP molecule is oriented along the long axis of the molecule from the naphthalene towards the BOP side. The transition moment components of Np-BOP and Per-BOP are listed in SI Figure S2. However, explaining the drop in the OS, in case of the Per-BOP, the NTOs localize on the perylene segment inspite of the maintained planarity (see Fig. 3). The transition dipole moment of the Per-BOP molecule is oriented along the perylene segment that is perpendicular to the long axis of the molecule connecting the Per to the BOP segments, explaining the drop in the OS.

We therefore proceed to consider means for extending the π-system such that the first excited state (S_1) remains delocalized across the whole conjugated system, and therefore discover potentially low gap and high fluorescence materials.

In this direction of increasing the conjugation of BOP-functionalized molecules we consider the Ph_2-NBOP and BisBOP-Np molecules introduced above in Fig. 1 and which have been synthesized and characterized spectroscopically[40,41]. Both these systems present red-shifted spectra and brighter luminescence compared to that of the Ph-BOP system [40,41]. The absorption maximum (λ_{abs}) of Ph_2-NBOP and BisBOP-Np is measured at 387 nm (3.21 eV) and 412 nm (3.01 eV), respectively. The emission peak (λ_{em}) is measured at 422 nm (2.94 eV) and 473 nm (2.62 eV). The spectroscopic data reveal that the λ_{abs} of BisBOP-Np is red-shifted by around 25 nm (0.20 eV) and 75 nm (0.67 eV) in comparison to that of Ph_2-NBOP and Ph-BOP, respectively [41]. The emission spectral peak of BisBOP-Np is red-shifted around 50 nm (0.32 eV) with respect to Ph_2-NBOP and Ph-BOP (the measured emission peak (λ_{em}) of Ph-BOP [39] is 425 nm (2.92 eV)).

The calculated excited states, listed in Table 2, correlate well with the observed spectral trends. The S_1 states are found to be dominated by the HOMO-LUMO replacements (H → L), see listed excited state properties in SI Table S1 for the absorption spectra and SI Table S2 for the emission spectra. For simplicity we consider BisBOP-Np systems where the *tert*-butyl (^{t}Bu) groups are replaced by capping hydrogen. The calculated Stokes shifts are 0.40 and 0.56 eV for Ph_2-NBOP and BisBOP-Np, respectively, which are only 0.2 eV larger than the measured values. The calculated absorption energy of BisBOP-Np is red-shifted by 0.37 and 0.62 eV, in comparison to that of Ph_2-NBOP and Ph-BOP, respectively. The calculated emission energy of BisBOP-Np is red-shifted by around 0.53 eV with respect to Ph_2-NBOP and Ph-BOP (the calculated emission energy of Ph-BOP[49] is 3.39 eV). The high OSs in these systems of the S_1 state at the excited state geometry explain well the observed bright luminescence. (The minor role of the substituting group in BisBOP-Np is confirmed by finding that the singlet and triplet excitation energies are only mildly affected by this substitution. The excited states of the simpler BisBOP-Np model (capping by hydrogens) are within 0.1 eV of those of Me-BisBOP-NP (capping by methyl groups). Compare excitation energies listed in SI Table S4 to those in Table 3.)

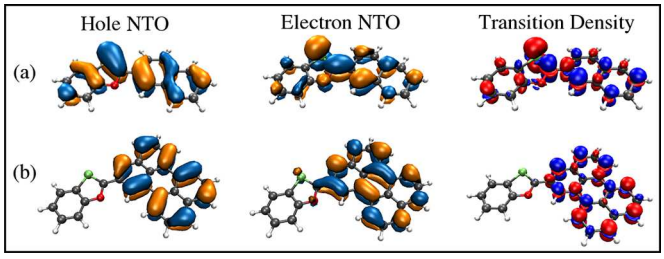

Fig. 3. The dominant pair of hole and electron NTOs and the transition density of the S_1 state of (a) Np-BOP and (b) Per-BOP molecules. Isovalue used for NTOs plot is 0.025 and for transition density plot is 0.002.

Table 2
Calculated absorption (E_{ab}) and emission (E_{em}) energies (eV), oscillator strengths (f), and fluorescence (k_{fl}) rate constants (sec^{-1}).

Molecule	E_{ab} (eV)	f	E_{em} (eV)	f	k_{fl}
Ph_2-NBOP	3.80	1.64	3.40	1.80	1.64×10^9
BisBOP-Np	3.43	2.15	2.87	2.29	1.39×10^9
FA-BOP	3.15	2.17	2.64	2.20	1.13×10^9

The λ_{abs} of Ph_2-NBOP[40] and BisBOP-Np[41] is measured at 387 nm (3.21 eV) and 412 nm (3.01 eV). The λ_{em} of Ph_2-NBOP and BisBOP-Np is measured at 422 nm (2.94 eV) and 473 nm (2.62 eV).

We next consider the proposed FA-BOP that is generated by adding two BOP units to the central naphthalene fragment of Ph_2-NBOP. Here we use an isomer of the synthesized Ph_2-NBOP molecule addressed above, [40] that is found to be energetically more stable and to enable planarity across the system. (See the isomers illustrated SI Figure S3.) In FA-BOP system, four arms are added symmetrically as shown in the insert of Fig. 4. The computed absorption energies of the first five singlet excited states are presented in the SI Table S1. The S_1 excitation in the FA-BOP system is confirmed to be of a HOMO to LUMO replacement, with a calculated Stokes shift of 0.51 eV. The absorption and emission energies of FA-BOP are red-shifted by 0.28 and 0.23 eV with respect to that of BisBOP-Np (Table 2). To highlight the role of the C═P doping of the conjugated system, we compare the excitation energy of a molecular system where all the C═P in FA-BOP are replaced by C═C bonds. Here the absorption and emission state energies are 0.3 eV higher at E_{ab}=3.42 eV (f=2.04) and E_{em}=2.92 eV, (f=2.15).

Importantly, both the ground state and emissive state geometries in FA-BOP are found to maintain an overall molecular planarity. In addition, the S_1 state is associated with delocalized NTOs, see Fig. 4. Consequently the OSs of the S_1 state in both emissive and ground state geometries remain similar or larger than those of the other synthesized molecules in the series (see Table 2). The hole and electron NTOs appear to be delocalized across the entire FA-BOP system. Importantly the NTOs present the same phase on the phenyl and BOP moieties shown to the left side of the central naphthalene fragment, and appear to be of opposite phase for the other half of the molecule. Consequently, in the transition

Table 3
Calculated vertical energy difference (eV) between S_1 and the excited triplet state at the S_1 geometry ($^1\Delta ST$), and the spin-orbit coupling element (cm^{-1}) ($V^{soc}_{T_m,S_1}$). (Additional triplet states energies are listed in the SI Table S3.).

Triplets	Ph_2-NBOP		BisBOP-Np		FA-BOP	
	$^1\Delta ST$	$V^{soc}_{T_m,S_1}$	$^1\Delta ST$	$V^{soc}_{T_m,S_1}$	$^1\Delta ST$	$V^{soc}_{T_m,S_1}$
T_1	-1.27	0.173	-1.16	0.202	-1.04	0.150
T_2	-1.14	0.164	-0.62	0.005	-0.35	0.003
T_3	**0.02**	**0.775**	**0.19**	**0.390**	-0.26	0.087
T_4	**0.22**	**0.779**	0.82	0.469	-0.21	0.005
T_5	0.54	0.128	0.97	0.646	**0.28**	**0.203**

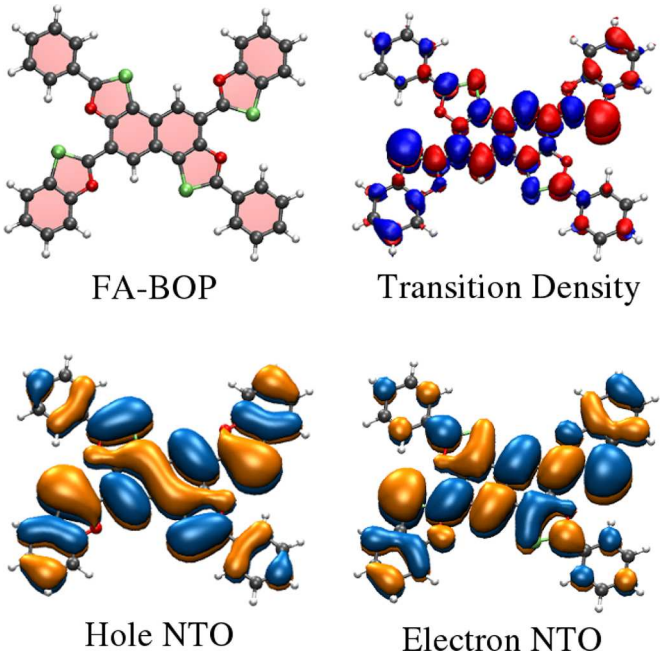

Fig. 4. The dominant pair of hole and electron NTOs and the transition density of the S_1 state of FA-BOP system. Isovalue used for NTOs plot is 0.01 and for transition density plot is 0.0007.

density (i.e, product of the NTOs), the positive poles (blue color) predominantly appear at the left side and the negative poles (red color) appear at the right side. The transition dipole moment in FA-BOP is strongly aligned along the axis connecting the BOP units. The calculated fluorescence rate constants (k_{fl}) are listed in Table 2. The fluorescence lifetimes are all in the *ns* time scale including for the Ph_2-NBOP for which a 1.04 *ns* S_1 lifetime was observed experimentally [40].

We next address the rates of competing nonradiative ISC processes. We summarize the calculated energy difference between S_1 and T_m states ($^1\Delta ST = E_{T_m} - E_{S_1}$) at the emissive geometry in Table 3. See also the illustration of the energy alignment in SI Figure S4. Both T_3 and T_4 states of Ph_2-NBOP are energetically close to the S_1 ($^1\Delta ST$ is 0.02 eV and 0.22 eV respectively). In the case of BisBOP-Np, only the T_3 state aligns energetically close to the S_1 state by 0.2 eV. The T_2 state is significantly lower resulting with $^1\Delta ST$ ~0.6 eV. The T_2-T_5 states of the FA-BOP system lie within the range of ±0.35 eV to the S_1 state. The key T_m states for the ISC are highlighted by bold font in Table 3. These states correspond to T_3 and T_4 for Ph_2-NBOP, T_3 for BisBOP-Np, and T_5 for FA-BOP, and are associated with both reasonable energy alignment and strong coupling with the S_1 state that is discussed next.

More specifically, the calculated spin-orbit coupling (SOC) elements ($V^{soc}_{T_m,S_1}$) between the S_1 and T_m states are listed in Table 3. The calculated SOC values tend to be small due to the symmetry of the states which are of the same character ($^3\pi\pi^*$) as of the S_1 state ($^1\pi\pi^*$) reflecting forbidden transition following El-Sayed's rules [73,74]. This trend is in contrast, for example, to sulfur-doped heterocyles (thiophene based systems), where the transition between $\pi\pi^*$ and $\pi\sigma^*$ state is associated with larger SOC values (> 1 cm^{-1}). The larger SOC is attributed to the geometrical distortion out of planarity due to the thiophene rings in the excited states [57]. The SOC value for both T_3 and T_4 states in Ph_2-NBOP is ~0.78 cm^{-1}, larger than for all other low energy states. In BisBOP-Np system the SOC value for T_3 state of 0.39 cm^{-1} is significantly larger than for the lower states, and where the higher states can be of even larger SOC but also with at least 0.8 eV higher energies. In the case of the FA-BOP system, the SOC value for the T_5 state, that is of energy that is only 0.2 eV higher than that of S_1, is 0.20 cm^{-1} The SOC values for T_2, T_3 and T_4 states in FA-BOP are negligible, while the T_1 is lower in energy by over 1 eV and therefore not relevant for ISC. The next state, T_6, is of high SOC with the S_1 but is of significant higher energy (0.7 eV) and therefore is not expected to play a role in the photophysics of the system. Therefore, the $S_1 \rightarrow T_3$ and $S_1 \rightarrow T_4$ in Ph_2-NBOP, $S_1 \rightarrow T_3$ in BisBOP-Np and $S_1 \rightarrow T_5$ in FA-BOP are the most important ISC channels.

We now consider the k_{isc} rates of the identified key transitions following the Marcus theory (Eq. (3)). The calculated energy parameters listed in Table 4 confirm that all the processes fall in the normal regime justifying the use of the semiclassical limit. For the $S_1 \rightarrow T_3$ channel of Ph_2-NBOP system $\Delta G < 0$ (downhill transition), whereas it is positive (uphill transition) for the $S_1 \rightarrow T_4$ channel. The calculated ISC rate constant for $S_1 \rightarrow T_3$ channel (2.12×10^8 s^{-1}) is larger than that for $S_1 \rightarrow T_4$ channel (2.90×10^7 s^{-1}). The ISC rate constant for the $S_1 \rightarrow T_3$ channel (2.35×10^7 s^{-1}) in BisBOP-Np is slower than for Ph_2-NBOP reflecting the SOC values. In the case of FA-BOP system, the ISC for $S_1 \rightarrow T_5$ channel (1.42×10^5 s^{-1}) is much slower compared to the others due to small SOC and uphill transition ($\Delta G > 0$). Importantly, in all the cases the ISC rate constants are significantly smaller than the fluorescence rate constants consistent with the observed bright fluorescence for Ph_2-NBOP and BisBOP-Np, and establishing a prediction of high fluorescence for FA-BOP.

4. Summary and concluding remarks

We consider doping conjugated skeletons by C=P bonds to achieve materials of reduced optical gap and high OS. We first benchmark our calculations of the luminescence properties by considering organic materials containing multiple benzoxaphosphole units, Ph_2-NBOP and BisBOP-Np molecules, which were successfully synthesized and analyzed spectroscopically [40,41]. Here we design a molecular conjugated system of multiple C=P bonds, the FA-BOP molecule, that is predicted to present strong luminescence and smaller optical gap than the parent materials. The FA-BOP consists of four-arms functionalizing a central naphtobisoxaphosphole (NBOP) unit with phenyl and BOP moieties.

Our calculations of R-BOP molecules confirm the expected trend, where increase of the conjugated skeleton lowers the gap while enhancing the OS. Here Per-BOP presents departure from this trend due to the localization of the electronic density. FA-BOP, the designed molecule, on the other hand, by preserving planarity is predicted to present a reduced optical gap and the highest OS of the molecules within the series. The calculated fluorescence rate corresponds to *ns* scale in lifetime. We also find that the potentially competing ISC rate is significantly smaller than the fluorescence rate. Ultimately, we predict that FA-BOP can function well as a molecular building block for polymers or covalent organic frameworks that may benefit light-emitting applications. This work represents a design approach to systematically achieve low-gap organic materials exhibiting enhanced fluorescence.

Supporting Information

Supplementary information of the consider molecular isomers Ph_2-NBOP and FA-BOP, excited state properties and excited state energies, and vertical energy difference and electronic coupling. The atomic co-

Table 4
Calculated intersystem crossing rate constants (k_{isc} in sec^{-1}) along with the relevant energy parameters $V^{soc}_{T_m,S_1}$ (cm^{-1}), ΔG (eV), λ (eV).

Molecule	$S_1 \rightarrow T_n$	$V^{soc}_{T_m,S_1}$	ΔG	λ	k_{isc}
Ph_2-NBOP	$S_1 \rightarrow T_3$	0.775	-0.503	0.525	2.12×10^8
	$S_1 \rightarrow T_4$	0.779	0.034	0.186	2.90×10^7
BisBOP-Np	$S_1 \rightarrow T_3$	0.390	-0.119	0.306	2.35×10^7
FA-BOP	$S_1 \rightarrow T_5$	0.203	0.136	0.148	1.42×10^5

ordinates of the studied molecules are also provided.

Declaration of Competing Interest

The authors declare that they have no known competing financial interests or personal relationships that could have appeared to influence the work reported in this paper.

Acknowledgements

SS gratefully thanks the National Institute of Technology, Tiruchirappalli, India, for the financial support through SEED grant and the DST-FIST scheme for funding through department. PD is thankful to the MHRD for her Junior Research Fellowship. JDP thanks the National Science Foundation (grant CHE-1955845) for funding. BDD is grateful for support by the Department of Energy (DOE), Basic Energy Sciences, the Chemical Sciences Geosciences and Biosciences Division, through Grant No. DE-SC0016501. We are also grateful to resource allocations on the Ohio Supercomputer Center [75] and the Kent State University, College of Arts and Sciences Computing Cluster.

Supplementary material

Supplementary material associated with this article can be found, in the online version, at 10.1016/j.jpap.2021.100089.

References

[1] O. Ostroverkhova, Organic optoelectronic materials: mechanisms and applications, Chem. Rev. 116 (2016) 13279–13412.
[2] Y. Shirota, Organic materials for electronic and optoelectronic devices, J. Mater. Chem. 10 (2000) 1–25.
[3] A.C. Grimsdale, K. Mullen, The chemistry of organic nanomaterials, Angew. Chem., Int. Ed. 44 (35) (2005) 5592–5629.
[4] M. Fahlman, S. Fabiano, V. Gueskine, D. Simon, M. Berggren, X. Crispin, Interfaces in organic electronics, Nat. Rev. Mater. 4 (2019) 627–650.
[5] S. Aiyer, R. Prasad, M. Kumar, K. Nirvikar, B. Jain, O.S. Kushwaha, Fluorescent carbon nanodots for targeted in vitro cancer cell imaging, Appl. Mater. Today 4 (2016) 71–77.
[6] C.W. Tang, S.A. van Slyke, Organic electroluminescent diodes, Appl. Phys. Lett. 51 (1987) 913–915.
[7] J.M. Burroughes, D. D. C. Bradley, A.R. Brown, A.N. Marks, K. Mackay, R. H. Friend, P.L. Burn, A.B. Holmes, Light-emitting diodes based on conjugated polymers, Nature 347 (1990) 539–541.
[8] A.C. Grimsdale, K.L. Chan, R.E. Martin, P.G. Jokisz, A.B. Holmes, Synthesis of light-emitting conjugated polymers for applications in electroluminescent devices, Chem. Rev. 109 (2009) 897–1091.
[9] R.W. Sinkledam, N.J. Greco, Y. Tor, Fluorescent analogs of biomolecular building blocks: design, properties, and applications, Chem. Rev. 110 (2010) 2579–2619.
[10] M.A. Baldo, M.E. Thompson, S.R. Forrest, High-efficiency fluorescent organic light-emitting devices using a phosphorescent sensitizer, Nature 403 (2000) 750–753.
[11] H. Uoyama, K. Goushi, K. Shizu, H. Nomura, C. Adachi, Highly efficient organic light-emitting diodes from delayed fluorescence, Nature 492 (2012) 234–238.
[12] Q. Zhang, B. Li, S. Huang, H. Nomura, H. Tanaka, C. Adachi, Efficient blue organic light-emitting diodes employing thermally activated delayed fluorescence, Nat. Photonics 8 (2014) 326–332.
[13] M. Cucchi, T. Matulaitis, N.A. Kukhta, J.V. Grazulevicius, S. Reineke, R. Scholz, Influence of the dielectric constant around an emitter on its delayed fluorescence, Phys. Rev. Appl. 12 (2019) 044021.
[14] B.S. Harrison, T.J. Foley, M. Bouguettaya, J.M. Boncella, J.R. Reynolds, K. S. Schanze, J. Shim, P.H. Holloway, G. Padmanaban, S. Ramakrishnan, Near-infrared electroluminescence from conjugated polymer/lanthanide porphyrin blends, Appl. Phys. Lett. 79 (23) (2001) 3770–3772.
[15] N. Tessler, V. Medvedev, M. Kazes, S. Kan, U. Banin, Efficient near-infrared polymer nanocrystal light-emitting diodes, Science 295 (2002) 1506–1508.
[16] L. Dou, Y. Liu, Z. Hong, G. Li, Y. Yang, Low-bandgap near-ir conjugated polymers/molecules for organic electronics, Chem. Rev. 115 (23) (2015) 12633–12665, https://doi.org/10.1021/acs.chemrev.5b00165.
[17] Z. Guo, S. Park, J. Yoon, I. Shin, Recent progress in the development of near-infrared fluorescent probes for bioimaging applications, Chem. Soc. Rev. 43 (2014) 16–29.
[18] J. Niu, Y. Wang, X. Zou, Y. Tan, C. Jia, X. Weng, L. Deng, Infrared electrochromic materials, devices and applications, Appl. Mater. Today 24 (2021) 101073.
[19] C. Duan, Y. Zhou, G.-G. Shan, Y. Chen, W. Zhao, D. Yuan, L. Zeng, X. Huang, G. Niu, Bright solid-state red-emissive BODIPYs: facile synthesis and their high-contrast mechanochromic properties, J. Mater. Chem. C 7 (2019) 3471–3478.
[20] I.M. Resta, J.F. Miravet, M. Yamaji, F. Galindo, Solid-state white-light emission from a pyrylium dye obtained in one synthetic step, J. Mater. Chem. C 8 (2020) 14348–14352.
[21] M.K. Bera, P. Pal, S. Malik, Solid-state emissive organic chromophores: design, strategy and building blocks, J. Mater. Chem. C 8 (2020) 788–802.
[22] S. Varughese, Non-covalent routes to tune the optical properties of molecular materials, J. Mater. Chem. C 2 (2014) 3499–3516.
[23] Q. Wan, Q. Huang, M. Liu, D. Xu, H. Huang, X. Zhang, Y. Wei, Aggregation-induced emission active luminescent polymeric nanoparticles: non-covalent fabrication methodologies and biomedical applications, Appl. Mater. Today 9 (2017) 145–160.
[24] H. Phillips, Z. Zheng, E. Geva, B.D. Dunietz, Orbital gap predictions for rational design of organic photovoltaic materials, Org. Electron. 15 (2014) 1509–1520.
[25] K. Begam, S. Bhandari, B. Maiti, B.D. Dunietz, Screened range-separated hybrid functional with polarizable continuum model overcomes challenges in describing triplet excitations in the condensed phase using TDDFT, J. Chem. Theory Comput. 16 (2020) 3287–3293.
[26] R. Davis, N. S. S. Kumar, S. Abraham, C.H. Suresh, N.P. Rath, N. Tamaoki, S. Das, Molecular packing and solid-state fluorescence of alkoxy-cyano substituted diphenylbutadienes: structure of the luminescent aggregates, J. Phys. Chem. C 112 (2008) 2137–2146.
[27] H. Lu, J. Mack, Y. Yang, Z. Shen, Structural modification strategies for the rational design of red/NIR region bodipys, Chem. Soc. Rev. 43 (2014) 4778–4823.
[28] Y. Yang, M.A. Mosquera, K. Skinner, A.E. Becerra, V. Shamamian, G.C. Schatz, M. A. Ratner, T.J. Marks, Electronic structure and potential reactivity of silaaromatic molecules, J. Phys. Chem. A 120 (2016) 9476–9488.
[29] M. Kobayashi, N. Hayakawa, T. Matsuo, B. Li, T. Fukunaga, D. Hashizume, H. Fueno, K. Tanaka, K. Tamao, (z)-1,2-di(1-pyrenyl)disilene: Synthesis, structure, and intramolecular charge-transfer emission, J. Am. Chem. Soc. 138 (2016) 758–761.
[30] N.M. Obeid, L. K. D. Maus, M. Zimmer, J. J. I. Bejan, A. J. P. White, V. Huch, G. Jung, D. Scheschkewitz, (oligo)aromatic species with one or two conjugated Si=Si bonds: near-IR emission of anthracenyl-bridged tetrasiladiene, Dalton Trans. 46 (2017) 8839–8848.
[31] R.C. Smith, J.D. Protasiewicz, Conjugated polymers featuring heavier main group element multiple bonds: a diphosphene-PPV, J. Am. Chem. Soc. 126 (2004) 2268–2269.
[32] R.C. Smith, J.D. Protasiewicz, Systematic investigation of PPV analogue oligomers incorporating low coordinate phosphorus centres, Eur. J. Inorg. Chem. 5 (2004) 998–1006.
[33] R.C. Smith, J.D. Protasiewicz, A fluorescent (e)-poly(p-phenylenephosphaalkene) prepared by a phospha-Wittig reaction, Inorg. Chem. 42 (2003) 5468–5470.
[34] V.A. Wright, B.O. Patrick, C. Schneider, D.P. Gates, Phosphorus copies of PPV: π-conjugated polymers and molecules composed of alternating phenylene and phosphaalkene moieties, J. Am. Chem. Soc. 128 (2006) 8836–8844.
[35] V.A. Wright, D.P. Gates, Poly(p-phenylenephosphaalkene): aπ conjugated macromolecule containing P=C bonds in the main chain, Angew. Chem. Int. Ed. 41 (2002) 2389–2392.
[36] X.-L. Geng, Q. Hu, B. Schafer, S. Ott, Phosphaalkenes in pi-conjugation with acetylenic arenes, Org. Lett. 12 (4) (2010) 692–695.
[37] J.C. Worch, D.N. Chirdon, A.B. Maurer, Y. Qiu, S.J. Geib, S. Bernhard, K.J. T. Noonan, Synthetic tuning of electronic and photophysical properties of 2-aryl-1,3-benzothiaphospholes, J. Org. Chem. 78 (2013) 7462–7469.
[38] J. A. W. Sklorz, S. Hoof, N. Rades, N.D. Rycke, L. Konczol, D. Szieberth, M. Weber, J. Wiecko, L. Nyulaszi, M. Hissler, C. Muller, Pyridyl-functionalised 3h-1,2,3,4-triazaphospholes: synthesis, coordination chemistry and photophysical properties of low-coordinate phosphorus compounds, Chem. Eur. J. 21 (2015) 11096–11109.
[39] M.P. Washington, V.B. Gudimetla, F.L. Laughlin, N. Deligonul, S. He, J.L. Payton, M.C. Simpson, J.D. Protasiewicz, Phosphorus can also be a photocopy, J. Am. Chem. Soc. 132 (2010) 4566–4567.
[40] F.L. Laughlin, N. Deligonul, A.L. Rheingold, J.A. Golen, B.J. Laughlin, R.C. Smith, J.D. Protasiewicz, Fluorescent heteroacenes with multiply-bonded phosphorus, Organometallics 32 (2013) 7116–7121.
[41] S. Wu, A.L. Rheingold, J.D. Protasiewicz, Luminescent materials containing multiple benzoxaphosphole units, Chem. Commun. 50 (2014) 11036–11038.
[42] S. Wu, N. Deligonal, J.D. Protasiewicz, An unusually unstable ortho-phosphinophenol and its use to prepare benzoxaphospholes having enhanced air-stability, Dalton Trans. 42 (2013) 14866–14874.
[43] F.L. Laughlin, A.L. Rheingold, N. Deligonul, B.J. Laughlin, R.C. Smith, L.J. Higham, J.D. Protasiewicz, Naphthoxaphospholes as examples of fluorescent phospha-acenes, Dalton Trans. 41 (2012) 12016–12022.
[44] M.P. Washington, J.L. Payton, M.C. Simpson, J.D. Protasiewicz, Redox behavior of 2-substituted 1,3-benzoxaphospholes and 2,6-substituted benzo[1,2-d:4,5-d] bisoxaphospholes, Organometallics 30 (2011) 1975–1983.
[45] E. Oberg, A. Orthaber, M.-P. Santoni, F. Howard, S. Ott, Toward metathesis reactions on vinylphosphaalkenes, Phosphorus Sulfur Silicon Relat. Elem. 188 (1–3) (2013) 152–158.
[46] B.W. Rawe, C.P. Chun, D.P. Gates, Anionic polymerisation of phosphaalkenes bearing polyaromatic chromophores: phosphine polymers showing turn-on emission selectively with peroxide, Chem. Sci. 5 (2014) 4928–4938.
[47] S. Wu, A.L. Rheingold, J.A. Golen, A.B. Grimm, J.D. Protasiewicz, Synthesis of a luminescent azaphosphole, Eur. J. Inorg. Chem. 2016 (5) (2016) 768–773.
[48] Y. Qiu, J.C. Worch, D.N. Chirdon, A. Kaur, A.B. Maurer, S. Amsterdam, C. R. Collins, T. Pintauer, D. Yaron, S. Bernhard, K. J. T. Noonan, Tuning thiophene with phosphorus: synthesis and electronic properties of benzobisthiaphospholes, Chem. A Eur. J. 20 (25) (2014) 7746–7751.

[49] S. Sarkar, J.D. Protasiewicz, B.D. Dunietz, Controlling the emissive activity in heterocyclic systems bearing C=P bonds, J. Phys. Chem. Lett. 9 (13) (2018) 3567–3572.
[50] J. Moon, M. Kim, J.S. Lim, J. Kim, Effect of phosphorus on the electronic and optical properties of naphthoxaphospholes: theoretical investigation, Mol. Phys. 116 (12) (2018) 1581–1588.
[51] H. Baek, J. Kim, TDDFT investigation of electronic and optical properties of diaryl-substituted naphtho[1,2-d:5,6-d']bis-(oxaphosphole) compounds, Comput. Theor. Chem. 1156 (2019) 12–19.
[52] J.R. Lakowicz, Radiative decay engineering: biophysical and biomedical applications, Anal. Biochem. 298 (2001) 1–24.
[53] N.J. Turro, V. Ramamurthy, J.C. Scaiano, Modern molecular photochemistry of organic molecules. University Science Books, Sausalito, California, 2010.
[54] R. Rossi, M. Ciofalo, A. Carpita, G. Ponterini, Singlet-triplet intersystem crossing in 2,2:5,2-terthiophene and some of its derivatives, J. Photochem. Photobiol. A: Chem 70 (1993) 59.
[55] B. Kraabel, D. Moses, A.J. Heeger, Direct observation of the intersystem crossing in poly(3-octylthiophene), J. Chem. Phys. 103 (1995) 5102.
[56] R.S. Becker, J.S.d. Melo, A.L. Macanita, F. Elisei, Comprehensive evaluation of the absorption, photophysical, energy transfer, structural, and theoretical properties of α-oligothiophenes with one to seven rings, J. Phys. Chem. 100 (1996) 48.
[57] D. Beljonne, Z. Shuai, G. Pourtois, J.L. Bredas, Spin-orbit coupling and intersystem crossing in conjugated polymers: a configuration interaction description, J. Phys. Chem. A 105 (2001) 3899–3907.
[58] S.J. Strickler, R.A. Berg, Relationship between absorption intensity and fluorescence lifetime of molecules, J. Chem. Phys. 37 (1962) 814.
[59] M.S. Kwon, J.H. Jordahl, A.W. Phillips, K. Chung, S. Lee, J. Gierschner, J. Lahannabcd, J. Kim, Multi-luminescent switching of metal-free organic phosphors for luminometric detection of organic solvents, Chem. Sci. 7 (2016) 2359–2363.
[60] P. Kimber, F. Plasser, Toward an understanding of electronic excitation energies beyond the molecular orbital picture, Phys. Chem. Chem. Phys. 22 (2020) 6058–6080.
[61] R.A. Marcus, Electron transfer reactions in chemistry. theory and experiment, Rev. Mod. Phys. 65 (1993) 599–610.
[62] Q. Ou, J.E. Subotnik, Electronic relaxation in benzaldehyde evaluated via TD-DFT and localized diabatization: intersystem crossings, conical intersections, and phosphorescence,, J. Phys. Chem. A 117 (2013) 19839–19849.
[63] S. Sarkar, H.P. Hendrickson, D. Lee, F. DeVine, J. Jung, E. Geva, J. Kim, B. D. Dunietz, Phosphorescence in bromobenzaldehyde can be enhanced through intramolecular heavy atom effect, J. Phys. Chem. C 121 (2017) 3771–3777.
[64] M.E. Casida, F. Gutierrez, J. Guan, F.-X. Gadea, D. Salahub, J.P. Daudey, Charge-transfer correction for improved time-dependent local density approximation excited-state potential energy curves: analysis within the two-level model with illustration for h_2 and lih, J. Chem. Phys. 113 (2000) 7062.
[65] M. J. G. Peach, M.J. Williamson, D.J. Tozer, Influence of triplet instabilities in TDDFT, J. Chem. Theory Comput. 7 (2011) 3578–3585.
[66] J.S. Sears, T. Koerzdoerfer, C.-R. Zhang, J.L. Brédas, Communication: orbital instabilities and triplet states from time-dependent density functional theory and long-range corrected functionals, J. Chem. Phys. 135 (2011) 151103.
[67] M. J. G. Peach, D.J. Tozer, Overcoming low orbital overlap and triplet instability problems in TDDFT, J. Phys. Chem. A 116 (2012) 9783–9789.
[68] J.-D. Chai, M. Head-Gordon, Systematic optimization of long-range corrected hybrid density functionals, J. Chem. Phys. 128 (2008) 084106.
[69] J.-D. Chai, M. Head-Gordon, Long-range corrected hybrid density functionals with damped atom-atom dispersion corrections, Phys. Chem. Chem. Phys. 10 (2008) 6615–6620.
[70] J.-D. Chai, M. Head-Gordon, Optimal operators for Hartree-Fock exchange from long-range corrected hybrid density functionals, Chem. Phys. Lett. 467 (2008) 176–178.
[71] C.D. Closser, O. Gessner, M. Head-Gordon, Simulations of the dissociation of small helium clusters with ab initio molecular dynamics in electronically excited states, J. Chem. Phys. 140 (2014) 134306.
[72] Y. Shao, Z. Gan, E. Epifanovsky, A.T. Gilbert, M. Wormit, J. Kussmann, A.W. Lange, A. Behn, J. Deng, X. Feng, D. Ghosh, M. Goldey, P.R. Horn, L.D. Jacobson, I. Kaliman, R.Z. Khaliullin, T. Ku, A. Landau, J. Liu, E.I. Proynov, Y.M. Rhee, R. M. Richard, M.A. Rohrdanz, R.P. Steele, E.J. Sundstrom, L.W. H III, P. M. Zimmerman, D. Zuev, B. Albrecht, E. Alguire, B. Austin, G.J.O. Beran, Y. A. Bernard, E. Berquist, K. Brandhorst, K.B. Bravaya, S.T. Brown, D. Casanova, C.-M. Chang, Y. Chen, S.H. Chien, K.D. Closser, D.L. Crittenden, M. Diedenhofen, A. D. R Jr., H. Do, A.D. Dutoi, R.G. Edgar, S. Fatehi, L. Fusti-Molnar, A. Ghysels, A. Golubeva-Zadorozhnaya, J. Gomes, M.W. Hanson-Heine, P.H. Harbach, A. W. Hauser, E.G. Hohenstein, Z.C. Holden, T.-C. Jagau, H. Ji, B. Kaduk, K. Khistyaev, J. Kim, J. Kim, R.A. King, P. Klunzinger, D. Kosenkov, T. Kowalczyk, C.M. Krauter, K.U. Lao, A.D. Laurent, K.V. Lawler, S.V. Levchenko, C.Y. Lin, F. Liu, E. Livshits, R.C. Lochan, A. Luenser, P. Manohar, S.F. Manzer, S.-P. Mao, N. Mardirossian, A.V. Marenich, S.A. Maurer, N.J. Mayhall, E. Neuscamman, C. M. Oana, R. Olivares-Amaya, D.P. O'Neill, J.A. Parkhill, T.M. Perrine, R. Peverati, A. Prociuk, D.R. Rehn, E. Rosta, N.J. Russ, S.M. Sharada, S. Sharma, D.W. Small, A. Sodt, T. Stein, D. Stck, Y.-C. Su, A.J. Thom, T. Tsuchimochi, V. Vanovschi, L. Vogt, O. Vydrov, T. Wang, M.A. Watson, J. Wenzel, A. White, C.F. Williams, J. Yang, S. Yeganeh, S.R. Yost, Z.-Q. You, I.Y. Zhang, X. Zhang, Y. Zhao, B. R. Brooks, G.K. Chan, D.M. Chipman, C.J. Cramer, A.G. W III, M.S. Gordon, W. J. Hehre, A. Klamt, F.S. H III, M.W. Schmidt, C.D. Sherrill, D.G. Truhlar, A. Warshel, X. Xu, A. Aspuru-Guzik, R. Baer, A.T. Bell, N.A. Besley, J.-D. Chai, A. Dreuw, B.D. Dunietz, T.R. Furlani, S.R. Gwaltney, C.-P. Hsu, Y. Jung, J. Kong, D. S. Lambrecht, W. Liang, C. Ochsenfeld, V.A. Rassolov, L.V. Slipchenko, J. E. Subotnik, T.V. Voorhis, J.M. Herbert, A.I. Krylov, P.M. Gill, M. Head-Gordon, Advances in molecular quantum chemistry contained in the q-chem 4 program package, Mol. Phys. 113 (2015) 184–215.
[73] S.K. Lower, M.A. El-Sayed, The triplet state and molecular electronic processes in organic molecules, Chem. Rev. 66 (1966) 199–241.
[74] M.A. El-Sayed, The triplet state. its radiative and nonradiative properties, Acc. Chem. Res. 1 (1968) 8–16.
[75] Ohio supercomputer center, 1987, http://osc.edu/ark:/19495/f5s1ph73 Accessed on 01.01.2014.